



Science Arts & Métiers (SAM)

is an open access repository that collects the work of Arts et Métiers Institute of Technology researchers and makes it freely available over the web where possible.

This is an author-deposited version published in: <https://sam.ensam.eu>
Handle ID: <http://hdl.handle.net/10985/7878>

To cite this version :

Marco PEDROTTI, Mohammad Ali MIRZAEI, Adrien TEDESCO, Simone BENEDETTO, Frédéric MERIENNE, Jean-Rémy CHARDONNET - Automatic Stress Classification With Pupil Diameter Analysis - International Journal of Human-Computer Interaction - Vol. 30, n°3, p.220-236 - 2014

Any correspondence concerning this service should be sent to the repository

Administrator : scienceouverte@ensam.eu



Automatic Stress Classification With Pupil Diameter Analysis

Marco Pedrotti^{1,2}, Mohammad Ali Mirzaei³, Adrien Tedesco⁴, Jean-Rémy Chardonnet³, Frédéric Mérienne³, Simone Benedetto^{2,5}, and Thierry Baccino^{2,5}

¹Université Paris 6 - Pierre et Marie Curie, France

²CHART/LUTIN (EA 4004), Paris, France

³Arts et Métiers ParisTech, Chalon-sur-Saône, France

⁴Scientific Brain Training, Villeurbanne, France

⁵Université Paris 8 - Vincennes St. Denis, France

This article proposes a method based on wavelet transform and neural networks for relating pupillary behavior to psychological stress. The proposed method was tested by recording pupil diameter and electrodermal activity during a simulated driving task. Self-report measures were also collected. Participants performed a baseline run with the driving task only, followed by three stress runs where they were required to perform the driving task along with sound alerts, the presence of two human evaluators, and both. Self-reports and pupil diameter successfully indexed stress manipulation, and significant correlations were found between these measures. However, electrodermal activity did not vary accordingly. After training, the four-way parallel neural network classifier could guess whether a given unknown pupil diameter signal came from one of the four experimental trials with 79.2% precision. The present study shows that pupil diameter signal has good discriminating power for stress detection.

1. INTRODUCTION

Stress detection and measurement are important issues in several human-computer interaction domains such as Affective Computing, Adaptive Automation, and Ambient Intelligence. In general, researchers and system designers seek to estimate the psychological state of operators in order to adapt or redesign the working environment accordingly (Sauter, 1991). The primary goal of such adaptation is to enhance overall system performance, trying to reduce workers' psychophysical detriment (e.g., Czaja & Sharit, 1993; Dennerlein, Becker, Johnson, Reynolds, & Picard, 2003; Fujigaki & Mori, 1997). One key aspect of stress measurement concerns the recording of physiological parameters, which are known to be modulated by the autonomic nervous system (ANS). However, despite

technological progress in biological signal acquisition, inferring psychological significance from physiological signals is still a major challenge as biological signal analysis has progressed less intensively (Cacioppo & Tassinari, 1990), and it can be stated that affect recognition has not reached a satisfying level yet (Mauss & Robinson, 2009; Van den Broek, Janssen, & Westerink, 2009).

This study describes a new method for stress measurement using pupil diameter (PD) signal analysis. It is well known that pupillometry is a reliable tool for studying cognitive and emotional processes (Granholm & Steinhauser, 2004; Kuhlmann & Böttcher, 1999). The pupil is the aperture of the iris, the pigmented structure containing two antagonistic muscle groups—the sphincter and the dilator muscles. The former constrict the pupil; the latter dilate the pupil. The human pupil is known to reflect the activity of the ANS: In particular, it has been shown that the pupil enlarges (mydriasis) as a consequence of mental effort exertion and various sources of psychological stress (see Beatty, 1982; Beatty & Lucero-Wagoner, 2000; Bradley, Miccoli, Escrig, & Lang, 2008; Goldwater, 1972; Partala & Surakka, 2003; Vo et al., 2008). After dilation, the pupil naturally tends to constrict (myosis) back to previous diameter. Thus, we formulated the hypothesis that overall pupillary activity (i.e., PD oscillations) should be more intense under stressful conditions: Phasic changes should follow stressful events. Moreover, mean signal amplitude should also increase, indicating higher tonic level.

However, the use of PD as a dependent variable in psychological studies has important methodological implications. The main concern stems from the primary function of the pupil itself, that is, the regulation of the amount of light that enters the retina. The so-called *light reflex* occurs to avoid overexposure and retinal damage (Loewenfeld & Lowenstein, 1993, p. 136). Such a constriction is rapid (latency within 250 ms from stimulus onset) and proportional to stimulus intensity, and it is affected by individual differences. The return to prestimulus diameter (*dark reflex*) is much slower

Address correspondence to Marco Pedrotti, CHART/LUTIN (EA 4004), Cité des Sciences et de l'Industrie de la Villette, 30 Avenue Corentin Cariou, Paris 75930, France. E-mail: marco.pedrotti@hotmail.it

Color versions of one or more of the figures in the article can be found online at www.tandfonline.com/hihc.

(see Beatty, 1986; Bergamin & Kardon, 2003; Ellis, 1981; Lanting et al., 1990). The *near reflex* (or accommodation response), that is, a near object requiring foveal focusing, causes pupil constriction, accompanied by eyes convergence and lenses curvature. Although this phenomena could regulate human pupil size from 1 up to 10 mm, very small (up to 0.01 mm) pupillary dilations can be elicited by various psychological manipulations (see Beatty & Lucero-Wagoner, 2000): The *psychosensory reflex* denotes pupil dilations evoked by sensory stimulation, whether auditory, tactile, gustatory, olfactory, or noxious. Beatty (1986) pointed out that this phenomenon is a sort of bridge between the well-understood *light* and *near* reflexes and the more complex pupillary variations associated with cognitive processing. Many other factors can lead to pupil diameter variations: Janisse (1977) identified 23 sources of pupil variation, to which the effect of verbalization (Bernick & Oberlander, 1968) could be added. Therefore, extreme care should be taken to control as many potential bias sources as possible. Among these, illumination requires particular attention, although most studies fail to report such measurements.

Bearing these considerations in mind, there is a substantial interest and potential benefit in using PD for stress detection in applied studies: Unlike other physiological measures (e.g., cardiovascular activity, electrodermal activity, electroencephalography, etc.), the pupil can be measured unobtrusively. With modern devices, one camera is sufficient for pupil tracking, and there is no need for physical contact. Remote eye trackers have such properties, and recent research has demonstrated their suitability for pupillometry studies (Klingner, Kumar, & Hanrahan, 2008; Palinko & Kun, 2010, 2011; Palinko, Kun, Shyrokov, & Heeman, 2012). Besides PD, other eye-movement metrics (e.g., saccade parameters) are known to reflect stress-related variations (see Benedetto, Pedrotti, & Bridgeman, 2011; Di Stasi, Catena, Cañas, Macknik, & Martinez-Conde, 2013). Efforts are also being made to unobtrusively measure skin temperature and other ANS measures with imaging techniques (see, e.g., Nhan & Chau, 2010; Shastri, Merla, Tsiamyrtzis, & Pavlidis, 2009).

The present study concerns stress detection in a simulated driving task. With the aim of validating our results by means of triangulation (Van den Broek et al., 2009), we recorded—besides PD—participants' self-reported stress levels and electrodermal activity (EDA; see section 3.5), a sensitive psychophysiological indicator of stress (Boucsein, 2012, p. 459).

The article is organized as follows: Existing PD data analysis techniques are introduced in section 1.1. Experimental setup and hypotheses of the present study are described in section 2. Section 3 describes the whole process of data acquisition and analysis. Statistical results are presented in section 4. The framework of automatic stress detection based on Wavelet-Neural Network is outlined in section 5: Wavelet multiresolution decomposition and Neural Networks

are used for feature extraction and classification, respectively. Classification results and future challenges are discussed in section 6.

1.1. Methods for PD Data Analysis

Over the last decades, several methods have been used for analyzing PD data. The signals coming from PD recordings have been analyzed in both the time and frequency domains: State-of-the art is briefly reviewed in this section. Regardless of the method employed for the analysis, eye-blink artifacts represent a common problem in video-pupillography: Most systems measure pupil size upon eye image processing (see Holmqvist et al., 2010; Wyatt, 2010). During eye-blinks the lid covers the eye, and the camera cannot detect the pupil. Because eye-tracking systems deal with this problem (loss of information) in a variety of ways (Gitelman, 2002), it is impossible to create a universal procedure to recover missing information. Several algorithms for eye-blink detection have been proposed, by both researchers directly interested in the eye-blink phenomenon and researchers faced with eye-blink artifacts (Pedrotti, Lei, Dzaack, & Rötting, 2011). Once blink onset and offset have been identified, missing/corrupted pupil data are usually estimated using linear (or cubic) interpolation, or even more sophisticated techniques such as moving average or support vector regression (see Nakayama, Yamamoto, & Kobayashi, 2012). Overall, pupil data preprocessing is necessary, because it is known that eye-blink artifacts have an impact on analysis results, both in the time and frequency domains (Nakayama, 2006; Nakayama & Shimizu, 2002, 2004).

The Task-Evoked Pupillary Response (TEPR) is a useful tool for PD signal analysis in the time domain. The main contributions on TEPR come from cognitive psychology. The rationale underlying this method is the same as the event-related potential (ERP) in electroencephalography (EEG) measurements. Because the magnitude of psychologically induced pupillary responses can be in the order of tenths—even hundredths—of millimeters, we can be more confident in associating such responses to a given stimulus if we know the exact time point of stimulus appearance. Like for event-related potentials, a time window (e.g., 500 ms) before stimulus onset is used as baseline, that is, the average PD \bar{x} for the prestimulus time window is calculated. Subsequently, \bar{x} is subtracted from each data point in the poststimulus time window (e.g., 5 s after stimulus onset). The resulting waveform—usually an average of several measurements (e.g., Figure 3A)—indicates the pupillary reaction to the stimulus, and parameters such as peak dilation and latency to the peak can be calculated. Beatty (1982) demonstrated that such parameters are sensitive indicators of processing load for different cognitive tasks. Although this technique is appropriate for laboratory studies implying short and simple tasks, several constraints might undermine its application in more complex and dynamic situations. Klingner (2010) introduced the fixation-aligned pupillary response averaging, in which eye fixations—instead of experimental stimuli—are used

to temporally align PD time windows. In addition, TEPRs have been analyzed using principal component analysis and independent component analysis in an attempt to reduce the large number of time points to a smaller set—usually two or three factors (see Granholm & Verney, 2004; Jainta & Baccino, 2010; Kuchinke, Vo, Hofmann, & Jacobs, 2007; Verney, Granholm, & Marshall, 2004).

To the authors’ knowledge, Lüdtke, Wilhelm, Adler, Schaeffel, and Wilhelm (1998) first introduced the use of Fast Fourier Transform for pupil signal analysis in the frequency domain. Analyzing a signal in such domain allows to know, for example, whether significant changes happen within specific frequency bands. With the aim of detecting low-frequency fatigue-related pupillary oscillations, Lüdtke and colleagues evaluated the mean value of the amplitude spectrum for all the frequencies at 0.8Hz or lower. Nakayama and Shimizu (2004) found that the power spectrum density of pupil signals increases within certain band intervals (0.1–0.5 Hz and 1.6–3.5Hz) as a function of cognitive task difficulty. Lew, Dyre, Werner, Wotring, and Tran (2008) analyzed PD signals using the Short-Time Fourier Transform, which allows to extract the frequency information yet preserving the time domain.

One promising technique for reducing data complexity in recorded PD signals is wavelet analysis. Marshall (2000, 2002) first proposed the use of wavelet analysis for analyzing PD time series, and associated the occurrence of high-frequency variations (faster than 20 ms, i.e., > 50Hz) to instances of cognitive load. Since then, to our knowledge, few studies have applied wavelet transforms to PD signals: Shi et al. (2006) analyzed pupillary behavior in relation to a user’s visual ability; Pinzon-Morales and Hirata (2012) evaluated PD oscillations to estimate sleepiness levels. In the present study, we used the Discrete Wavelet Transform (DWT) as a tool to extract relevant signal features (i.e., low-frequency approximation), discarding the noise that appears in the high-frequency part of the signal (see section 3.4.4). In this respect, our approach is opposite to the one proposed by Marshall.

2. METHOD

2.1. Stimuli

Our rationale for stress manipulation implies the repeated performance of a simple driving task, to which we added

different external stressful stimuli (see section 2.3). The protocol was approved by the French National Board of Informatics and Freedom (declaration n. 0727429; <http://www.cnil.fr>). Participants performed a simulated Lane Change Test (LCT), which consists of driving on a traffic-free straight three-lane road (see Figure 1A), changing lanes according to the information appearing on two identical road signs displayed concurrently every 150 m, on both sides of the road (ISO, 2010; Minin, Benedetto, Pedrotti, Re, & Montanari, 2011; Mitsopoulos-Rubens, Trotter, & Lenné, 2011).

The driving simulator consisted of seat (Playseat Evolution), steering wheel and pedals (Logitech G25, no gear-shift was used), and a 32-in. LCD monitor (Thomson 32LB220B4, 70 × 39cm, 1366 × 768px). The LCT software (<http://www.corys.com>) limited the maximum speed at 60 km/hr, so that participants could maintain this speed by simple flat-out. Each trial consisted of 18 lane changes, accomplished over 180 s (ISO, 2010). The average distance between participant and screen was 130 cm.

2.2. Participants

Thirty-three healthy people (all with valid driving license) participated in the experiment. Seventeen people were allocated to the *experimental* group, that is, the group that underwent stress manipulation, and the remaining 16 were assigned to the *control* group (see section 2.3). The experimental group contained nine women (M age = 38 years, SD = 15) and eight men (M age = 43 years, SD = 9). Eight women (M age = 42 years, SD = 8) and eight men (M age = 41 years, SD = 13) were assigned to the control group. All participants read and signed an informed consent and received a reward for every hour spent inside the laboratory. Participants were informed that they could leave the experiment at any time and for any reason. One participant from the control group quit the experiment during t_2 because of simulator sickness.

Participants’ stress trait was measured with the State-Trait Anxiety Inventory (STAY-B; Spielberger, Gorsuch, Lushene, Vagg, & Jacobs, 1983, translated in French by Schweitzer & Paulhan, 1990). To disclose possible social desirable responding, we asked participants to fill in the Social Desirability Scale (DS36; Tournois, Mesnil, & Kop, 2000). The experimental and control groups did not differ in terms of STAY-B

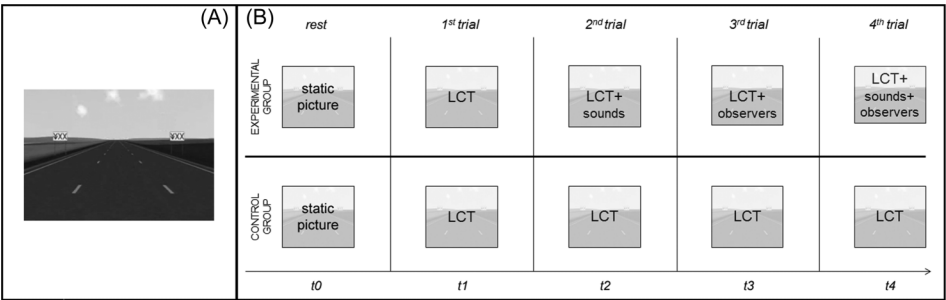


FIG. 1. (A) Lane Change Test scenario. (B) Experimental design.

scores, $t(30) = 1.03$, *ns*, or on DS36 scores, $t(30) = 0.1$, *ns*, for self-deception, and $t(30) = 0.23$, *ns*, for other-deception.

2.3. Experimental Design and Procedure

Upon arrival at the lab, participants sat in a quiet room wherein they installed the electrodes for electrodermal measurement on their forehead (see section 3.5), read and signed an informed consent, and filled in the STAY-B and DS36 questionnaires (see section 2.2). Thereafter, participants moved to the simulation room, where they received onscreen instructions for the LCT (see ISO, 2010, Annex A) and performed a 1-min LCT training to disclose any potential issue (misunderstandings, simulator sickness, technical equipment, etc.).

Before beginning the LCT sessions, we recorded baseline physiological signals during a 90-s rest period (t_0) in which participants looked at a static picture of the LCT scenario. Subsequently, participants carried out four LCT trials (Figure 1B). The control group performed the four driving trials without any disturbing factor. The experimental group underwent two types of stressors, announced by means of screen instructions displayed before the LCT trial started.

Before the second trial (t_2), participants were informed that they would hear a sound if their driving behavior was not appropriate (i.e., beginning a lane change as soon as the symbols appear on a sign, but not before; see ISO, 2010, Annex A). Indeed, a sound was presented every 20 s, regardless of driving behavior. To avoid excessive habituation, three different sounds were used: A 8.6 Hz white noise, a police siren, and a 4 KHz tone (.wav files are available from the corresponding author). All sounds lasted 1 s, and they were presented in a pseudorandom order: each sound was presented three times, totaling nine sound presentations in the second trial.

Before the third trial (t_3), participants were informed that their driving performance would have been evaluated by two experts. After this announcement, two experimenters entered the test room. These “fake” experimenters (one man and one woman) wore white lab coats, they held a copybook which they used for taking notes, and they stood on the participant’s right (90° of visual angle) so that their presence could be perceived without disturbing the execution of the driving task. Moreover, a previously floor-pointed camera was turned toward the participant, so that she or he would believe she or he was being filmed. No stressful sounds were presented during the third trial.

Before the fourth trial (t_4), participants were informed that they would have been evaluated by the experimenters and alerted with sounds in case of incorrect driving behavior.

After each LCT trial, participants reported their perceived stress level (see section 3.3). Each trial lasted 3 min.

2.4. Hypotheses

For the experimental group, stress level should be lowest at t_1 —where simple LCT performance is demanded—and highest at t_4 , where two concurrent stressors are associated with the

LCT task. We cannot predict whether stress level will significantly differ between t_2 and t_3 , that is, we do not know a priori whether alert sounds are more stressful than observers (or vice versa). What we know is that they are two different types of stressors, and they could be then classified.

For the control group, we expect stress level to significantly decrease from t_1 to t_4 as an effect of habituation.

The two groups should exhibit the same stress level at t_1 , as they bear exactly the same conditions until that point. We expect to find significant between-groups differences at t_2 , t_3 , t_4 .

We expect PD changes to reflect increased stress levels for the experimental group and decreased stress levels for the control group. Electrodermal and self-report measures are expected to correlate with pupillary behavior measures.

3. DATA ACQUISITION AND ANALYSIS

3.1. Apparatus Synchronization

The equipment used in the present study includes an eye tracker (RED 4, <http://www.smivision.com>) for PD measurement, an A/D converter (MP36R, <http://www.biopac.com>) for measuring illumination and EDA, a PC for stimulus (LCT) presentation, and a PC running Matlab (<http://www.mathworks.com>) for synchronization and auditory stimulus delivery (psychtoolbox.org; Brainard, 1997; Kleiner, Brainard, & Pelli, 2007; Pelli, 1997). All the systems were connected on a local area network, and synchronization was achieved using a combination of custom software written in Matlab and free software (synergy-foss.org). Each single experimental event (e.g., beginning of a LCT trial, presentation of a LCT sign, presentation of a sound, etc.) was marked—via TCP/IP messages—in the eye tracker’s and A/D converter’s log files for conjoint offline analysis. A detailed technical description goes beyond the scope of the present article, and interested readers may refer to the corresponding author for further information.

3.2. Illumination

Illumination was measured with an Extech 403125 luxmeter (<http://www.extech.com>). With the aim of recording the amount of light that impacted on the participant’s eyes, the light sensor was attached to a ceiling-mounted holder, placed 5 cm above the participant’s head, laterally centered with respect to her or his nose. The luxmeter was connected to a Biopac MP36R A/D converter which stored illumination values in *lux* at 50Hz sampling rate.

3.3. Visual Analog Scale

After each LCT trial (t_1 , t_2 , t_3 , t_4) participants rated their perceived stress level using three on-screen visual analog scales (VASs). The VAS ranged from 0 (*not at all*) to 100 (*maximum*). The three dimensions were *stress* (“How much stress were you feeling during task performance?”), *anxiety* (“How much anxiety were you feeling during task performance?”), and *avoidance*

TABLE 1
Correlations Between VAS Dimensions

	anxiety t_1	anxiety t_2	anxiety t_3	anxiety t_4	avoidance t_1	avoidance t_2	avoidance t_3	avoidance t_4
stress t_1	.93**				.13			
stress t_2		.87**				.76**		
stress t_3			.95**				.51**	
stress t_4				.61**				.74**
anxiety t_1					.18			
anxiety t_2						.66**		
anxiety t_3							.52**	
anxiety t_4								.37*

Note. $N = 32$ (one participant quit the experiment after t_2 because of simulator sickness).

* $p < .05$. ** $p < .005$.

(“During task performance, to what extent were you willing to leave the situation?”). Correlation analysis revealed strong correlations between the three dimensions, except between *stress* t_1 and *avoidance* t_1 , and between *anxiety* t_1 and *avoidance* t_1 (see Table 1).

3.4. Pupil Diameter

PD was recorded at 50Hz sampling rate using a SMI RED 4 remote video eye tracker. This system measures pupil size and eye movements by means of pupil and corneal reflection tracking (see Holmqvist et al., 2010), and has a precision of 0.01 mm for PD. PD signal was treated according to the following procedure:

- Step 1. Preprocessing: Eye-blink artifacts were identified and replaced by linear interpolation (see section 3.4.1).
- Step 2. TEPRs extraction: Pupillary responses following sound presentations (in t_2 and t_4) were evaluated to confirm the existence of pupillary reactions to stressful stimuli (see section 3.4.2).
- Step 3. Normalization: PD values in t_1 , t_2 , t_3 , t_4 were normalized for each participant, according to her or his average PD at rest (see section 3.4.3).
- Step 4. Analysis of variance (ANOVA): We tested the hypothesis that our stress manipulation had an effect on average PD (see section 4.2).
- Step 5. Signal approximation extraction: The normalized PD signals from t_1 , t_2 , t_3 , t_4 were transformed by means of DWT. The Haar wavelet was used to decompose and transfer the signal into multiresolution representation (see section 3.4.4).
- Step 6. Classification with neural networks: PD signal approximation was used as an input vector (feature) during the training and test stages (see section 5).

The first step (Preprocessing) is generally necessary regardless of the aim of any study. Concerning our study, we consider steps 2 and 4 (TEPRs extraction, ANOVA) mandatory for

theoretically justifying the use of PD as a stress index, as they demonstrate the sensitivity of PD to stress manipulations. Normalization (step 3) is necessary because each person has her or his own PD at rest. Steps 5 and 6 (Signal approximation extraction and Classification) are an attempt to use PD for automatic stress measurement in applied contexts. With the aim of being able to measure stress levels over relatively short periods, we extracted and analyzed (in steps 4, 5, and 6) only the first 80s of PD data from each trial.

3.4.1. Pupil diameter preprocessing. The RED 4 provides two types of pupil measurement: (a) in pixel and (b) in millimeters (Figure 2). In the present study, millimeter values were preferred for PD signal analysis because they are calculated taking into account the distance between participant and camera, providing more reliable data than raw pixel measurement. Nonetheless, the RED 4 outputs useful information for blink detection in the pixel data. When a blink occurs, zeros—along with other physiologically impossible values—are recorded in the pixel output (see Figure 2, bottom line, right-hand scale). In a statistical perspective, such values can be considered as outliers of the PD distribution of a given data set. Blinks were detected as contiguous sets of outliers. Moreover, other blink markers in the eye-tracking protocol—such as the momentary loss of gaze position during blink—were combined to foster correct blink detection percentage (for a detailed description of the algorithm, see Pedrotti et al., 2011). Blink onset was defined as the third sample (60 ms) preceding the first zero observation: At this point, the lid starts its descent until the pupil is covered (in 79% of blinks; see Pedrotti et al., 2011). Blink offset was defined as the first valid sample after a blink: At this point, the pupil is visible to the eye tracker camera.

After identifying blink onsets and offsets in the pixel data, we replaced blink data in the millimeter output by means of linear interpolation, using blink onset as starting point, and two samples after blink offset as ending point. An example of the result of this preprocessing procedure is shown in Figure 2 (top line, left-hand scale).

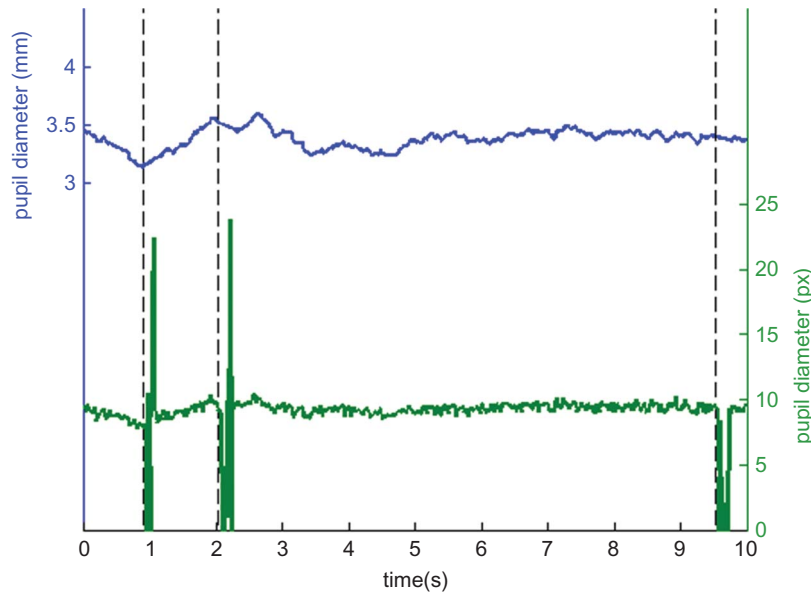


FIG. 2. Pupil output in mm (top line, left-hand scale) and px (bottom line, right-hand scale). *Note.* Dashed vertical lines indicate blink onsets.

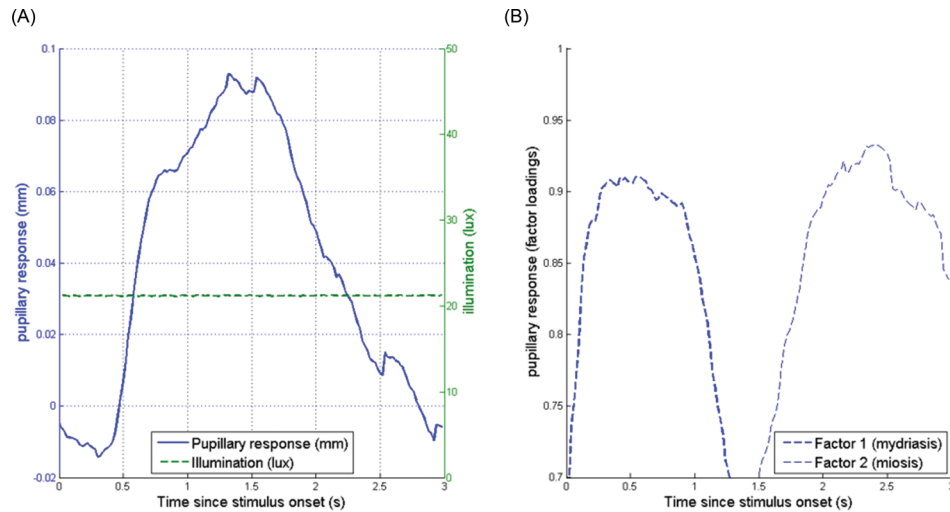


FIG. 3. (A) Pupillary response to stressful sounds (solid line, left-hand scale) under constant illumination (dashed line, right-hand scale). (B) Pupillary response factor loadings (only loadings > 0.7 are considered for interpretation).

3.4.2. Task-Evoked Pupillary Responses. TEPRs were extracted—from the experimental group—for each sound presentation in t_2 and t_4 (see Figure 1B and section 2.3). Baseline pupil diameter was computed as the mean PD in the 200-ms prestimulus time window. Figure 3A shows the average pupillary response (solid line, left-hand scale) from 288 waveforms (16 participants¹ \times 9 sounds \times 2 trials). The dashed line (right-hand scale) shows the average illumination, measured in synchrony with PD (see section 3.1). A typical phasic pupillary reaction—dilation (mydriasis) followed by

constriction (myosis)—occurred. With the aim of reducing the 150 data points (50 points \times 3 s, 50Hz sampling rate) to a smaller set of factors, the data from the 288 TEPRs extracted were analyzed with a factor analysis using Statistica (<http://www.statsoft.com>). The 150 data points were treated as dependent variables serving as input for factor analysis. Factor loadings were extracted following a varimax rotation. Two factors could explain 82.34% of variance in the data, that is, pupillary response shapes are consistent across individuals and trials. Factor loadings plotted against time (Figure 3B) clearly show the separation between the rising (factor 1, mydriasis, 62.91% of explained variance) and falling (factor 2, myosis, 19.43% of explained variance) part of the pupillary response

¹One participant's data were excluded because of poor recording quality.

depicted in Figure 3A. Moreover, the absence of measured relevant illumination changes allows us to associate the recorded waveform to the stress elicited by experimental manipulation (sound delivery associated with poor driving performance).

3.4.3. Pupil diameter normalization. The TEPR does not require previous data normalization, as the baseline PD is recalculated for each event, based on a short prestimulus time window (200 ms in our case): This procedure can be viewed as a sort of normalization, in that a participant- and moment-specific PD value is subtracted from absolute PD values. However, before performing any interindividual comparison (such as an ANOVA), PD values should be normalized, as it is known that PD at rest differs between people. For each participant, we calculated mean PD (μPD_{t_0}) at rest (t_0 in Figure 1B). Subsequently, μPD_{t_0} was subtracted from each PD data point in t_1, t_2, t_3, t_4 . This procedure allows for later comparisons of PD between participants.

3.4.4. Signal approximation extraction. Combination of wavelet and neural networks has been accepted as an accurate method for feature extraction and classification (Minu, Lineesh, & Jessy John, 2010). Any noisy signal imposes some uncertainty to the calculation and, consequently, to the results. Therefore, before using PD signal as input for the neural network classifier, we need to remove noise from the signal. Denoising could improve classification performance, as it would increase the signal-to-noise ratio. Moreover, it would reduce computational costs, that is, a shorter time to obtain results: This latter aspect is important in a real-time application perspective, although we focus on offline analysis for the present study.

Several mathematical approaches could be used for this purpose: We chose the DWT because (a) it allows removing noise yet preserving the original shape of the signal and (b) it encompasses a down-sampling procedure, which reduces computation time.

Mathematically, a signal (time series) $x(t) \in L(R)$ can be decomposed into linear combination of a set of n base functions $\{\phi_0, \phi_1, \dots, \phi_n\}$ if the signal is in the space spanned by the basis. Then, $x(t)$ can be decomposed into a linear combination of the base functions (Mallat, 1989):

$$x(t) = \sum_k a_k \phi_k(t) \quad k < n \quad (k < \infty), k \in \mathbb{Z} \quad (1)$$

where k is an integer index of the finite or infinite sum and $a_k, \phi_k(t)$ are expansion coefficients and functions, respectively. This representation is the most common form of multispectrum decomposition. Consider two sets of base functions:

1. $\phi_{j,k}(t) = 2^{-\frac{j}{2}} \phi(2^{-j}t - kx), j > 0, k \in \mathbb{Z}$
2. $\phi_k(t) = e^{\frac{2\pi k t}{T}}$

If Item 1 or 2 are substituted in Equation 1, the wavelet and Fourier decompositions will be achieved, respectively. These are two well-known examples of decomposition of a signal into

primitive or fundamental constituents of their spaces. In fact, the Fourier series decomposes a signal into a set of sine and cosine functions. By DWT in multiresolution analysis, a signal is represented by a sum of a set of more flexible functions called *mother wavelet*, which are localized both in time and frequency.

Any wavelet decomposition consists of two parts: approximation and detail. Approximation refers to the overall, general form of the signal (e.g., low-frequency component), whereas detail better explains the high-frequency information such as edges, discontinuities, sharp points, and so on. Approximation and detail coefficients of a given discrete signal $x[n]$ can be extracted by low-pass and high-pass filtering, respectively. Figure 4B shows an example of signal approximation extraction using the Haar wavelet as mother wavelet, and five decomposition levels (i.e., the output of level_{*n*} is used as input for level_{*n+1*}). It seems evident that approximation preserves the original shape of the signal, whereas noise is discarded: In most cases, noise resides in the high-frequency part (Hamid, Nawi, & Ghazali, 2011). In the original signal (Figure 4A) 4,000 data points (coefficients) are needed to describe 80 s of pupil diameter (sample rate is 50Hz). Each wavelet decomposition level encompasses a down-sampling by a 2 factor. After five decompositions, sampling rate is reduced from 50Hz to 1.5625Hz, and 125 coefficients are sufficient to describe 80 s of pupil diameter. The vectors containing the 125 coefficients will be used as input for a neural network classifier (see section 5).

3.5. Electrodermal Activity

Skin conductance (SC) was recorded using the exosomatic method with Direct Current (Boucsein, 2012). Two Biopac EL507 disposable circular electrodes (Ag/AgCl, 1cm diameter circular contact area, 0.5% Chloride) were attached to the participant's forehead. Although palmar and plantar zones would be preferable for EDA recording, as they have higher sweat glands density (Dawson, Schell, & Fillion, 2000; Sato, Kang, Saga, & Sato, 1989), the driving task employed in the present study required both hands and feet to be completely free. The electrodes were fixed to the skin upon participant's arrival at the lab, assuring a minimum delay of 15 min before the recordings started. This time is sufficient to allow good electrical contact between the skin and the electrode surface. An elastic headband was used to prevent artifacts due to wire movements (Boucsein et al., 2012). The electrodes were connected to the Biopac MP36R A/D converter (50Hz sampling rate). For the EDA recording channel, a low-pass filter was applied (35Hz cutoff frequency). SC signals were treated with the following procedure:

- Step 1. Filtering: A low-pass filter was applied, with 2Hz cutoff frequency.
- Step 2. Down-sampling: Sampling rate was reduced from 50Hz to 10Hz.
- Step 3. Transformation: Data were transformed with the formula $y = \log(I + x)$ (Boucsein, 2012). The respective units are labeled as log μS .

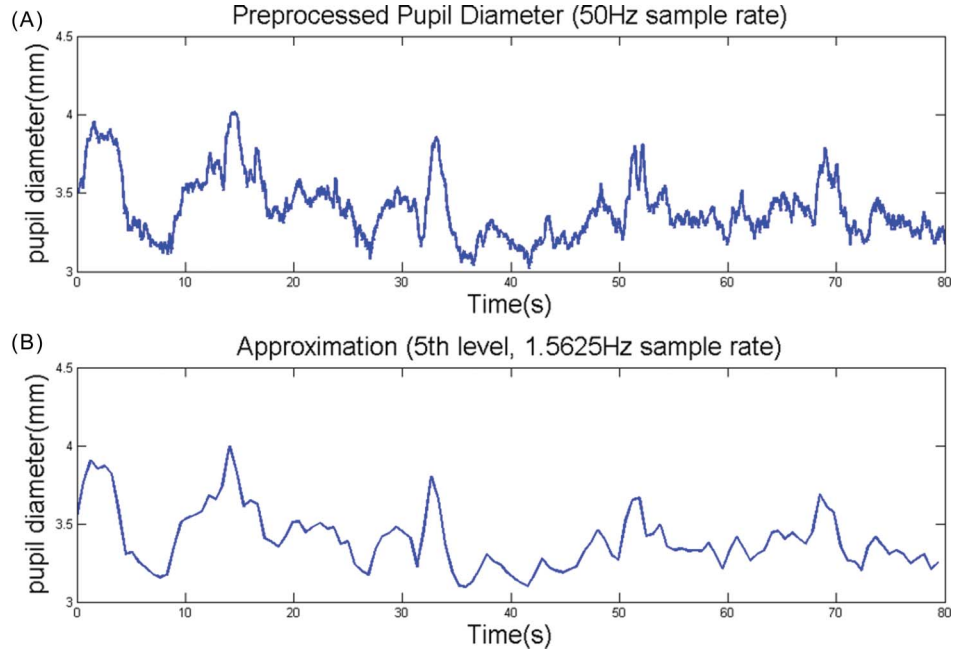


FIG. 4. (A) Preprocessed pupil diameter from trial t_2 of Participant 7. (B) Signal approximation after five wavelet (Haar) decomposition levels.

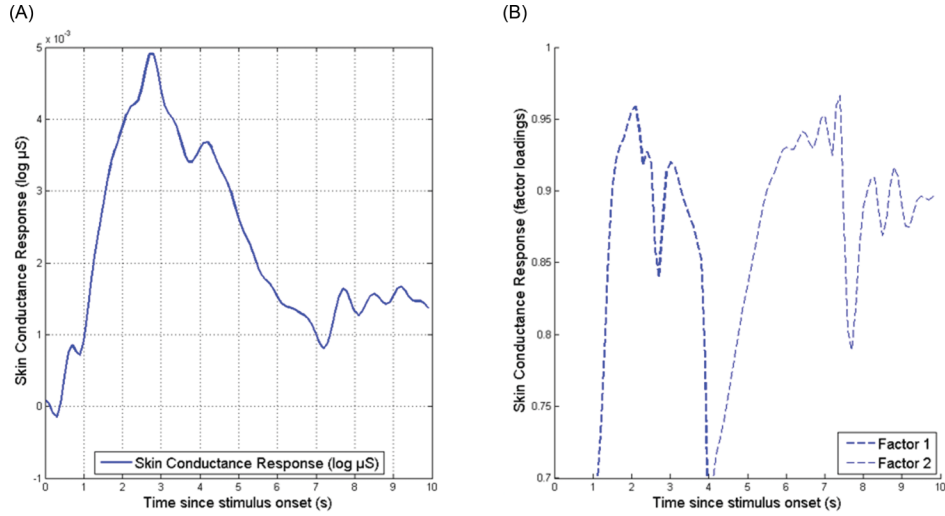


FIG. 5. (A) Skin Conductance Response to stressful sounds. (B) Skin Conductance Response factor loadings (only loadings > 0.7 are considered for interpretation).

Step 4. SC Response (SCR) extraction: SCRs were extracted following sound presentations in t_2 and t_4 (experimental group). The average SC in the 200-ms prestimulus time window was subtracted from each SC data point in the 10-s poststimulus time window. Figure 5A shows the average SCR from 288 sound presentations (16 participants² \times 9 sounds \times 2 trials). Like for PD data (see section 3.4.2), we used SCR time-series as input for factor analysis: Two

factors could explain 75.52% of variance (54.24% Factor 1, 21.28% Factor 2). Figure 5B shows factor loadings plotted against time. Unlike for TEPRs, the temporal separation between the two factors (roughly at 4 s) does not match the peak of the average SCR (Figure 5A): Factor interpretation is harder in this case; however, the overall proportion of explained variance tells that SCRs, like TEPRs, have a uniform structure across participants and trials.

Step 5. Non-Specific Electrodermal Response Frequency (NS.EDR freq.) extraction (see section 4.3.1)

Step 6. EDA Area extraction (see section 4.3.2)

²One participant was excluded because of too many artifacts in the SC record.

4. RESULTS

4.1. Visual Analog Scale

VAS *stress* scores from 32 participants³ were analyzed with a repeated-measures ANOVA (rmANOVA) using *trial* (t_1 , t_2 , t_3 , t_4) as within-factor and *group* (experimental, control) as between-factor (see Figure 6). A Trial \times Group interaction effect was found, $F(3, 90) = 5.41$, $p < .005$, $\eta^2_p = .15$. The effect of group is also significant, $F(1, 30) = 7.25$, $p < .05$, $\eta^2_p = .19$, with higher scores for the experimental group.

The difference on VAS *stress* scores between the experimental and control group is not significant at t_1 , $F(1, 30) = 0.03$, ns . VAS *stress* scores are significantly higher for the experimental group at t_2 , $F(1, 30) = 10.06$, $p < .005$, $\eta^2_p = .25$; t_3 , $F(1, 30) = 7.79$, $p < .01$, $\eta^2_p = .21$; t_4 , $F(1, 30) = 5.64$, $p < .05$, $\eta^2_p = .16$.

A *trial* effect, $F(3, 48) = 4.6$, $p < .01$, $\eta^2_p = .22$, was found within the experimental group: VAS *stress* scores are significantly higher at t_2 with respect to t_1 , $F(1, 16) = 8.72$, $p < .01$, $\eta^2_p = .35$; at t_3 with respect to t_1 , $F(1, 16) = 9.78$, $p < .01$, $\eta^2_p = .38$; at t_4 with respect to t_1 , $F(1, 16) = 4.46$, $p = .05$, $\eta^2_p = .22$. The differences between t_2 and t_3 , t_2 and t_4 , t_3 and t_4 are not significant.

Within the control group, there is no *trial* effect.

4.2. Pupil Diameter

Before carrying out any between-groups comparison at t_1 , t_2 , t_3 , t_4 , we verified that average PD at rest (t_0) did not differ between the experimental and control groups. Preprocessed

³One participant quit the experiment after t_2 because of simulator sickness.

average PD was calculated for 16 participants of the experimental group (one participant was excluded because of poor recording quality) and for 13 participants of the control group (two participants were excluded because of poor recording quality, and one participant was excluded because she quit the experiment after t_2). The data were analyzed in an independent samples t test, which confirmed no difference on average PD at t_0 between the two groups, $t(27) = 1.52$, ns .

We then tested the hypothesis that stress manipulation had an effect on mean PD across the experimental trials t_1 , t_2 , t_3 , t_4 . Normalized average pupil diameters were calculated for the experimental group (16 participants; one was excluded because of poor recording quality) and the control group (13 participants; two were excluded because of poor recording quality, one was excluded because she quit the experiment after t_2) at t_1 , t_2 , t_3 , t_4 . Data were analyzed with a rmANOVA, using *trial* (t_1 , t_2 , t_3 , t_4) as within-factor and *group* (experimental, control) as between factor. A significant Trial \times Group interaction effect was found, $F(3, 81) = 9.14$, $p < .001$, $\eta^2_p = .25$ (see Figure 7). The effect of group was also present, $F(1, 27) = 4.01$, $p = .05$, $\eta^2_p = .13$, in that normalized average pupil diameter was higher for the experimental with respect to the control group. When t_1 was removed from the within factors (as stress manipulation effectively started at t_2), the effect of group emerged more clearly, $F(1, 27) = 6.31$, $p < .05$, $\eta^2_p = .19$.

There was no difference between the experimental and control group at t_1 , $F(1, 27) = 0.05$, ns , whereas PD was significantly larger for the experimental group at t_2 , $F(1, 27) = 6.93$, $p < .05$, $\eta^2_p = .2$; t_3 , $F(1, 27) = 5.35$, $p < .05$, $\eta^2_p = .16$; t_4 , $F(1, 27) = 5.31$, $p < .05$, $\eta^2_p = .16$.

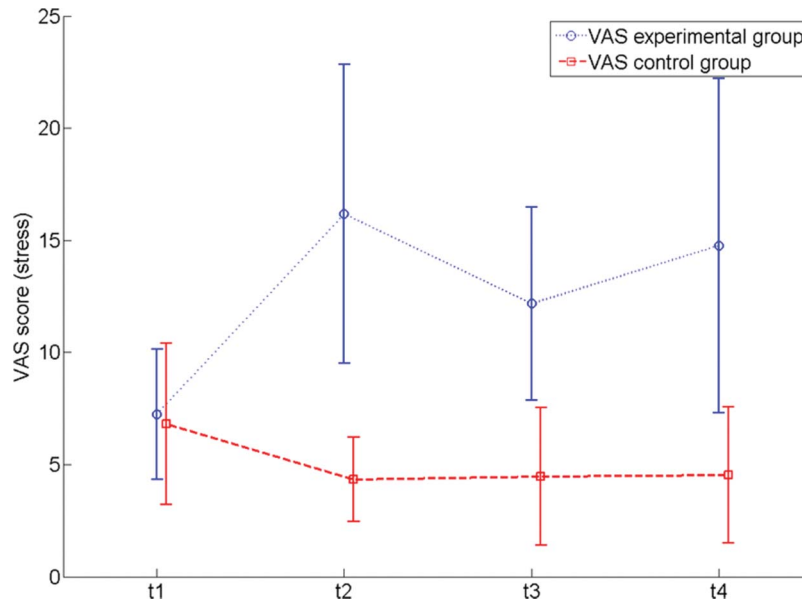


FIG. 6. Average VAS scores (*stress* dimension) for each group and experimental trial. Note. Vertical bars denote 95% confidence intervals (mean \pm 2SE). $N = 32$ (17 experimental + 15 controls).

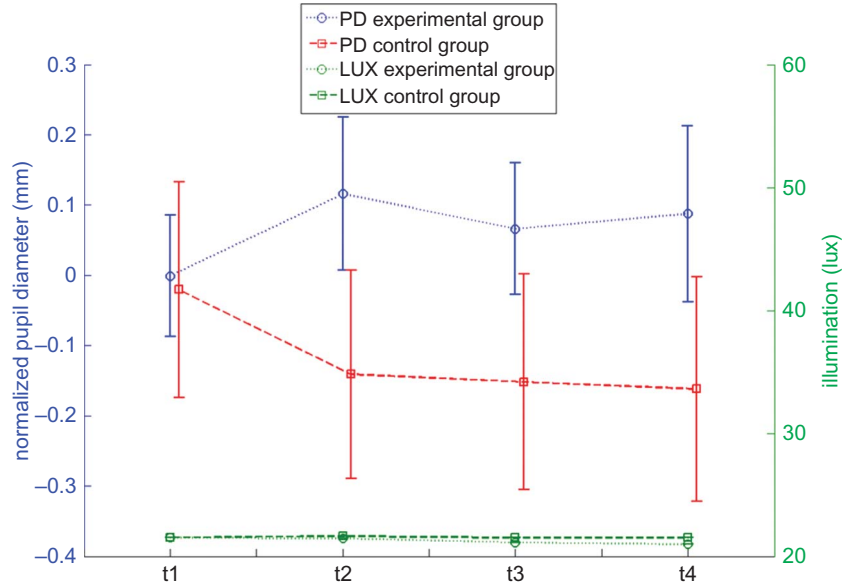


FIG. 7. Normalized average pupil diameter (left-hand scale) and average illumination (right-hand scale) for each group and experimental trial. *Note.* Vertical bars denote 95% confidence intervals (mean \pm 2SE). $N = 29$ (16 experimental + 13 controls).

The effect of trial was significant, $F(3, 45) = 3.45$, $p < .05$, $\eta^2_p = .19$, within the experimental group: PD was significantly larger at t_2 with respect to t_1 , $F(1, 15) = 12.63$, $p < .005$, $\eta^2_p = .46$; t_3 with respect to t_1 , $F(1, 15) = 7.42$, $p < .05$, $\eta^2_p = .33$. The differences between t_1 and t_4 , t_2 and t_3 , t_2 and t_4 , t_3 and t_4 were not significant.

Within the control group, the effect of trial was significant, $F(3, 36) = 7.22$, $p < .001$, $\eta^2_p = .37$: PD significantly decreased at t_2 with respect to t_1 , $F(1, 12) = 7.7$, $p < .05$, $\eta^2_p = .39$; at t_3 with respect to t_1 , $F(1, 12) = 13.74$, $p < .005$, $\eta^2_p = .53$; at t_4 with respect to t_1 , $F(1, 12) = 12.83$, $p < .005$, $\eta^2_p = .52$. The differences between t_2 and t_3 , t_2 and t_4 , t_3 and t_4 were not significant.

4.3. Electrodermal Activity

4.3.1. Nonspecific Electrodermal Response Frequency. NS.EDR freq., that is, the number of SCRs in absence of apparent stimulation, is thought to be an indicator of negatively tuned emotional states such as stress (Boucsein, 2012), in that NS.EDR freq. should increase under stressful conditions. NS.EDR freq. scores were analyzed with an rmANOVA using trial (t_1 , t_2 , t_3 , t_4) as within factor and group (experimental, control) as between factor. No significant effects were found.

4.3.2. EDA area. The area (computed as time-integral) below a SC waveform can be used as a measure of emotional arousal (see Bach, Friston, & Dolan, 2010; Boucsein, 2012). Because SC level has great interindividual variability, we subtracted the estimated tonic level from each SC time series before computing area measures. Tonic level was estimated by means of deconvolution using the Ledalab package (Benedek

& Kaernbach, 2010; <http://www.ledalab.de>). Figure 8A shows an example of the tonic-level estimation used in this study. The SC waveform—after subtraction of the estimated tonic level—shows a zero baseline (Figure 8B), making it possible to compare SC between individuals. These SC vectors were used as input for calculating area scores on a trial-by-trial basis. Areas were calculated by trapezoidal numerical integration using the Matlab *trapz* function. Area scores were then analyzed with an rmANOVA using trial (t_1 , t_2 , t_3 , t_4) as within factor and group (experimental, control) as between factor. No significant effects were found.

4.4. Bivariate Analysis

4.4.1. Correlation between subjective and physiological measures. It appears that normalized average VAS and PD scores have a similar pattern across the experimental trials, for both the experimental and control groups (see Figures 6 and 7). For the experimental group, both stress measures show a steep increase at t_2 with respect to t_1 , followed by a decrease at t_3 . Finally, another increase occurs at t_4 . For the control group, both measures decrease at t_2 and maintain a relatively stable level until t_4 . Significant correlations were found between normalized average PD and VAS stress scores at t_1 ($r = .4$, $p < .05$), t_2 ($r = .41$, $p < .05$), t_3 ($r = .44$, $p < .05$), and t_4 ($r = .4$, $p < .05$).

4.4.2. Correlation between PD and illumination. Illumination is an important factor influencing PD (see section 1). In this experiment, both stimulus and ambient illumination were kept constant during the whole experiment. Despite this, illumination data analysis revealed a slight illumination decrease for the experimental group at t_3 and t_4 (see Figure 7). Postexperiment investigations revealed that the cause

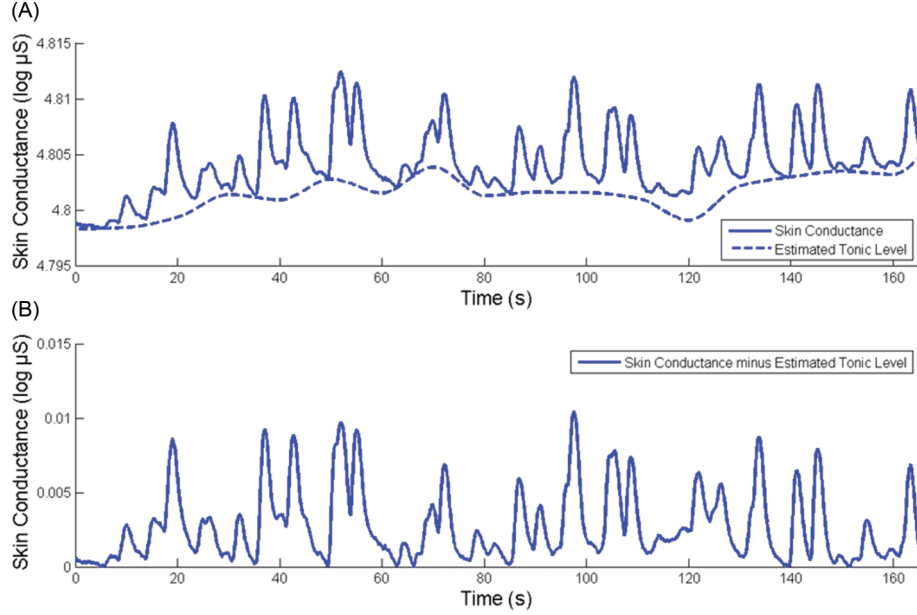


FIG. 8. (A) Skin conductance (solid line) and tonic level (dashed line) estimated by deconvolution (Benedek & Kaernbach, 2010). (B) Skin conductance minus tonic level, showing a zero baseline. The time-integral of this time series is used as EDA area measure.

could be attributed to the presence of the “fake” experimenters in the test room. Any displacement in the test room—even apparently insignificant ones like removing a chair—could cause an illumination change, indexed by the high sensitivity of the luxmeter. Although such subtle changes are below visual threshold and could not influence pupil size (Loewenfeld & Lowenstein, 1993), we tested whether normalized average PD was correlated with average illumination at t_1 , t_2 , t_3 , t_4 . No significant correlations were found.

5. CLASSIFICATION OF PD WITH NEURAL NETWORKS

After verifying the sensitivity of PD to stress manipulations (see section 4.2), we used PD signal approximation as input for a classifier. Statistical analyses support our choice of PD as a stress measure, in that average PD is significantly larger for the experimental group—with respect to the control group—at t_2 , t_3 , t_4 , whereas there is no difference at t_1 . This is in line with our predictions, as there was no stress manipulation until the end of t_1 , that is, the two groups were exactly in the same conditions before t_2 . Further support for this consideration comes from the subjective stress ratings (VAS; see section 4.1).

The aim of this analysis stage is automatic stress classification using normalized pupil diameter as the only information source: for this purpose, we use only PD data from the experimental group, that is, the group that underwent stress manipulation.

Following our experimental plan (Figure 1B), four classes should be used—one class for t_1 , one class for t_2 , one class for t_3 , and one class for t_4 . The hypothesis underlying the experimental plan was that participants in the experimental

group would feel more stressed as the experiment went on, with t_4 being the most stressful trial because of the cumulative effect of stressful sounds and human observers. Indeed, statistics revealed that PD significantly increased only at t_2 and t_3 with respect to t_1 , that is, differences between the different types of stressors (sound at t_2 , observation at t_3 , and their combination at t_4) could not be revealed using statistical linear models (see section 4.2). Such statistics rely on mean and variance as basic features for discrimination. In contrast, neural networks have a nonlinear characteristic, which is imposed by nonlinear transfer functions such as *logsig*, *tansig*, and so on. Such a more sophisticated classifier could improve discrimination performance using the whole signal (or its approximation) as input. Specifically, PD signal approximations (see section 3.4.4) were used as input features for classification.

The classification procedure involves two stages. In Stage 1 (training), four binary neural network classifiers are trained. Each of these classifiers operates in *one-versus-all* mode, that is, the aim of the training here is to maximize recognition precision of one class with respect to all the other classes (e.g., maximize recognition of t_1 with respect to t_2 , t_3 and t_4).

In Stage 2 (test), the four binary classifiers are put in parallel. An unknown, unlabeled PD signal approximation \vec{x}' is given as input to each of the four binary classifiers. Each classifier returns a score y (between 0 and 1), which can be interpreted as the probability that \vec{x}' belongs to a certain class (i.e., the degree to which an instance is a member of a class; see Fawcett, 2006). The final decision is made according to the highest score attributed to \vec{x}' by each of the four binary classifier.

Data from 10 participants (randomly selected) were used in the training stage (10 participants \times 4 classes, totaling

40 signals). Data from the remaining six participants were used in the test stage (6 participants \times 4 classes, totaling 24 signals). Implementation details are outlined in the following sections.

5.1. Binary Classifiers Architectures

Figure 9 shows a schematic representation of the *one-versus-all* classification procedure: an 80-s artifact-free PD signal \vec{x} (preprocessed normalized PD) is decomposed by means of DWT (see section 3.4.4) using the Haar mother wavelet. Signal approximation \vec{x}' is extracted and given as input to a binary neural network classifier. The classifier returns a score y . In an ideal situation, the binary classifier “ t_1 vs. t_2, t_3, t_4 ” (i.e., the classifier specialized for recognizing PD signals coming from t_1 trials) assigns a score $y = 1$ to an input signal \vec{x}' recorded during a t_1 trial, and a score $y = 0$ to an input signal \vec{x}' recorded during a t_2 , t_3 , or t_4 trial.

Table 2 summarizes architectural details of the four *one-versus-all* binary classifiers.

5.2. Binary Classifiers Training

Each of the four binary classifiers was trained separately using the Matlab Neural Network Training tool (*nn toolbox*). The Levenberg-Marquardt algorithm, which updates weight and bias values according to gradient descent and other conjugate gradient methods (Moré, 1978), was selected. Parameter values are reported in Table 3.

5.3. Four-Way Parallel Classifier Architecture

Figure 10 depicts the scheme of the four-way parallel classification procedure. An unknown, unlabeled PD signal approximation \vec{x}' (i.e., \vec{x}' has never been used in the training stage) is given as input to each of the four binary classifiers. Each classifier returns a score y . Scores are stored in the 4-D vector \vec{y} . In the example in Figure 10, the binary classifier “ t_1 vs. t_2, t_3, t_4 ” assigned a score of 0.9 to \vec{x}' . All the scores assigned to \vec{x}' from the other binary classifiers are lower than 0.9; thus we conclude that \vec{x}' comes from a t_1 trial.

5.4. Four-Way Parallel Classifier Test

Data from six participants were used for test, totaling 24 (6 participants \times 4 classes) signal approximations \vec{x}' . The four-way parallel classifier has a precision of 79.2%, that is, five misclassifications out of 24 signals. Detailed confusion matrix is shown in Table 4.

6. DISCUSSION

Among several psychophysiological correlates of stress—such as cardiovascular activity, electrodermal activity, respiration—we focused on PD because it can be measured in a completely unobtrusive manner. This makes PD particularly attractive in a real-life implementation perspective, where stress level could be measured automatically, by using video cameras. We proposed a method for relating PD behavior to psychological stress and tested its validity in a simulated driving experiment. For ethical reasons, experimental stressors

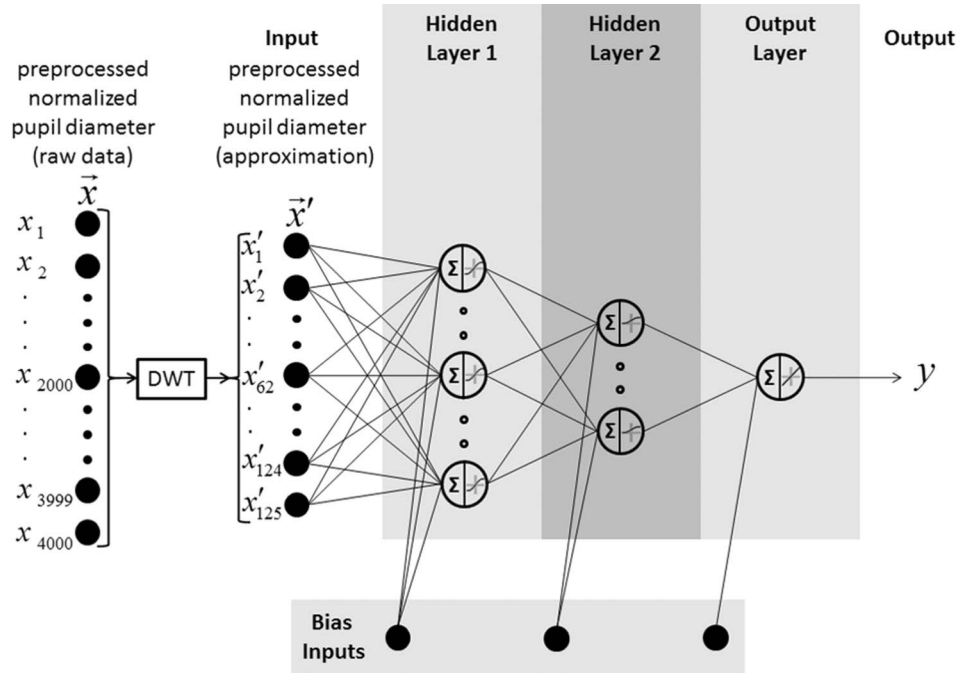


FIG. 9. Schematic representation of the *one-versus-all* binary neural network classifier.

TABLE 2
Neural Network Classifiers Architectures

Network	Hidden Layer I No. of Neurons	Hidden Layer I Transfer Function	Hidden Layer II No. of neurons	Hidden Layer II Transfer Function	Output Layer No. of Neurons	Output Layer Transfer Function
$t1$ vs. $t2, t3, t4$	15	tan-sigmoid	8	log-sigmoid	1	pureline
$t2$ vs. $t1, t3, t4$	14	tan-sigmoid	7	log-sigmoid	1	pureline
$t3$ vs. $t1, t2, t4$	11	tan-sigmoid	6	log-sigmoid	1	pureline
$t4$ vs. $t1, t2, t3$	11	tan-sigmoid	6	log-sigmoid	1	pureline

Note. Architecture details of the four binary classifiers (see Figure 9). Each classifier is designed to maximize recognition of one class with respect to all the other classes (e.g., maximize recognition of t_1 with respect to t_2, t_3, t_4).

TABLE 3
Parameter Values of the Neural Network Training Algorithm

Parameter	epochs	time	goal	$grad_{min}$	μ	μ_{dec}	μ_{inc}	μ_{max}
Value	1000	infinite	0	1e-08	0.001	0.1	10	1e10

Note. $epochs$ = maximum number of iterations; $time$ = time limit before algorithm stops; $goal$ = target gradient value; $grad_{min}$ = minimum gradient magnitude; μ = convergence factor (see Barman & Chowdhury, 2012).

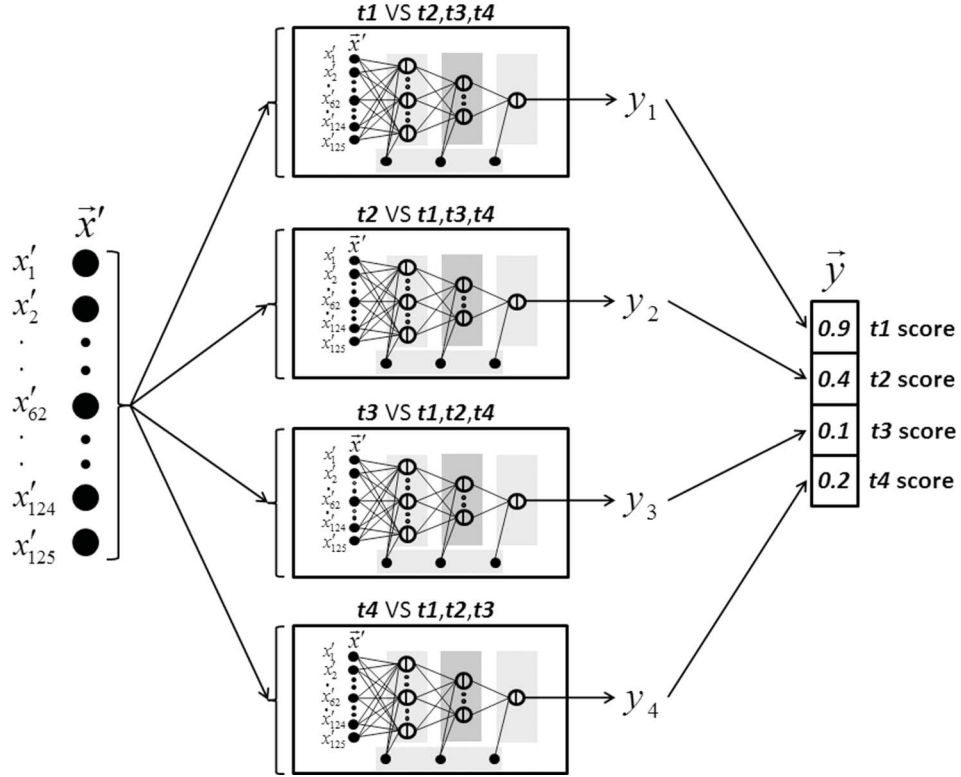


FIG. 10. Schematic representation of the four-way parallel neural network classifier.

TABLE 4
Four-Way Classifier Confusion Matrix

	Predicted			
	t1	t2	t3	t4
Actual				
t1	66.7% (4)	0	33.3% (2)	0
t2	0	83.3% (5)	0	16.7% (1)
t3	0	0	83.3% (5)	16.7% (1)
t4	0	16.7% (1)	0	83.3% (5)

Note. Numbers in parentheses indicate frequencies.

were conceived to elicit moderate stress levels, as confirmed by subjective ratings (VAS) results (see Figure 6). The fact that PD could index such mild variations is encouraging for further developments in which higher stress levels could be detected.

We proved the sensitivity of PD as a stress concomitant, in both event-related and general state paradigms. For the event-related part, we showed how pupillary responses (TEPRs) follow the presentation of auditory stimuli associated with poor task performance: Participants in the experimental group were told that they would hear a sound alert if their driving behavior was not appropriate. Because of the simplicity of the driving task (LCT), participants were expected to feel disoriented, irritated, frustrated at every sound presentation: During t_2 and t_4 they performed exactly the same driving task as t_1 , with the exception that sounds alerts occurred every 20 s regardless of driving performance. Thus, the TEPR reflects momentary stressful stimuli delivery, given that the exact time point of stimulus presentation is known. This technique is useful for basic research in controlled experiments, but it requires high control because every task-relevant event needs to be marked for offline analysis. In more naturalistic environments, tasks can have complex structures: Stressful events might not be predictable and localized in time a priori. Moreover, the small magnitude of the TEPR (roughly 0.1 mm as in Figure 3A) makes it particularly prone to confounding factors such as measurement noise and other sources of pupillary variation. For applied contexts, a valuable stress assessment method should be blind to both the temporal occurrence of stressors and the structure of the task.

The TEPR issues could be partially overcome using a more general-state measure (i.e., normalized average PD). This measure was influenced by the experimental manipulation as well. If we look at between-groups comparisons (i.e., experimental vs. control), normalized average PD is definitely a powerful discriminator because it significantly increased at t_2 , t_3 , and t_4 . Furthermore, it showed no between-groups difference at t_1 ,

confirming its reliability. For within-groups analysis, however, discrimination becomes more challenging, as we are looking for subtle differences between stress induced by sounds and human observers (and combination of both), and we don't know a priori which one is more stressful: Within the experimental group, significant differences were found only between the nonstress trials (t_1) and stress trials (t_2 , t_3); that is, we could not discriminate between t_2 and t_3 , t_2 and t_4 , t_3 and t_4 . Moreover, although average PD is higher at t_4 with respect to t_1 (see Figure 7), the difference is not statistically significant: Two factors could explain this. First, humans are likely influenced by habituation: At t_4 , participants have already had some experience with both *sounds* (since t_2) and *observers* (since t_3); thus it is reasonable that they feel less stressed at t_4 . Moreover, at t_4 they perform the LCT for the fourth time, which should also lower the stress induced by the LCT itself. We suggest that habituation (to both the LCT and the stressors) played a major role than the summation of two stressors (these two stressors are no more a novelty at t_4). Second, we are dealing with linear statistical models (ANOVA) and it should be clear that psychophysiological phenomena cannot be completely described in this domain.

With the aim of improving discrimination performance in a real-life oriented context, we devised an automated classifier. The results provided by the classifier are promising, yet we underline that they come from PD data recorded under controlled illumination. Designing such an autonomous stress measurement system, which relies solely on a short period of a time series (or a real-time signal), raises at least one question: What would happen if the level of noise increases, for example, because of environmental effects? In the case of PD, we can regard environmental illumination as a major noise source. Because in our experiment illumination was controlled, we cannot answer this question with empirical evidence. Neural networks were essentially inspired from studies of brain structure (Widrow, Gupta, & Maitra, 1973), and they are known to be remarkably tolerant to noise in input data. However, further research is needed to integrate—in our system—pupillary light reflex information, which could be estimated by measuring illumination and other factors (e.g., Watson & Yellot, 2012).

Concerning EDA measures, we obtained contrasting results: Event-related concomitants of stressful sounds (i.e., SCRs) were found, and factor analysis confirmed their relatively stable response behavior (75.52% of explained variance with two factors). However, NS.EDR freq.—an indicator of adverse emotional states in human-computer interaction (Boucsein, 2012)—did not return the expected results, in that it did not increase with stress level. It is known that NS.EDR freq. calculation can provide different results depending on event-detection algorithms: Overlapping SCRs are likely, especially in applied contexts such as the present experiment. We tried to overcome this problem by extracting an area measure of EDA, but the results remain unclear: It might be that the stress level in our experiment is too low—according to subjective

measures—to be indexed by electrodermal measures. Another possible and more “technical” explanation could be the fact that we placed the electrodes on the participants’ foreheads—because of experimental constraints (i.e., driving task)—instead of using palms and soles as recording sites: Dawson et al. (2000) suggested that emotion-evoked sweating is more evident in palmar and plantar zones because of higher sweat gland density (600/cm² for palms, 700/cm² for soles, 181/cm² for the forehead; see Sato et al., 1989). Finally, recent studies suggested that EDA signals have less discriminating power—compared to PD signals—for stress classification (Ren, Barreto, Gao, & Adjouadi, 2013; Zhai & Barreto, 2006).

Subjective ratings showed moderate yet significant correlations with normalized average PD. Although this result is encouraging, we remark that relying only on ANS measures is not the key for automatic stress measurement. A widely accepted perspective states that emotions are organized according to two principal dimensions, that is, arousal and valence (Mauss & Robinson, 2009). The former ranges from states of low activation (e.g., calm) to states of high activation (e.g., excited), whereas the latter counters positively tuned states (e.g., happy) versus negatively tuned ones (e.g., angry). Whereas ANS measures are known to be reliable indexes of arousal, they don’t give us indications about valence (see, e.g., Janisse, 1977). Thus, pupil diameter could increase because of positive stress (eustress) or negative stress, in the same way. In the present study, we examined the valence dimension by means of subjective ratings. However, this requires some active intervention by the user’s side, which is not suitable for an automatic stress measurement system. In this perspective, automatic valence indexes will be investigated in future research, with particular attention toward facial expressions: Like for PD, these measures can be acquired unobtrusively by using video cameras.

FUNDING

This research was supported by the French Minister of Economy, Finances and Industry, under contract n. F1105041V (MASSAI).

ACKNOWLEDGEMENT

We thank the anonymous reviewers for their helpful comments.

REFERENCES

- Bach, D. R., Friston, K. J., & Dolan, R. J. (2010). Analytic measures for quantification of arousal from spontaneous skin conductance fluctuations. *International Journal of Psychophysiology*, 76, 52–55. doi:10.1016/j.ijpsycho.2010.01.011
- Barman, D., & Chowdhury, N. (2012). A method for movie business prediction using back-propagation neural network. *International Journal of Information Technology and Computer Science*, 11, 67–73. doi:10.5815/ijitcs.2012.11.09
- Beatty, J. (1982). Task-evoked pupillary responses, processing load, and the structure of processing resources. *Psychological Bulletin*, 91, 276–292. doi:10.1037/0033-2909.91.2.276
- Beatty, J. (1986). The pupillary system. In M. G. H. Coles, E. Donchin, & S. W. Porges (Eds.), *Psychophysiology: Systems, processes, and applications* (pp. 43–50). New York, NY: Guilford.
- Beatty, J., & Lucero-Wagoner, B. (2000). The pupillary system. In J. T. Cacioppo, L. G. Tassinary, & G. G. Berntson (Eds.), *Handbook of psychophysiology* (2nd ed., pp. 142–162). Cambridge, UK: Cambridge University Press.
- Benedek, M., & Kaernbach, C. (2010). A continuous measure of phasic electrodermal activity. *Journal of Neuroscience Methods*, 190, 80–91. doi:10.1016/j.jneumeth.2010.04.028
- Benedetto, S., Pedrotti, M., & Bridgeman, B. (2011). Microsaccades and exploratory saccades in a naturalistic environment. *Journal of Eye Movement Research*, 4(2), 1–10.
- Bergamin, O., & Kardon, R.H. (2003). Latency of the pupil light reflex: sample rate, stimulus intensity, and variation in normal subjects. *Investigative Ophthalmology & Visual Science*, 44, 1546–1554. doi:10.1167/iovs.02-0468
- Bernick, N., & Oberlander, M. (1968). Effect of verbalization and two different modes of experiencing pupil size. *Perception & Psychophysics*, 3, 327–330. doi:10.3758/BF03212478
- Boucsein, W. (2012). *Electrodermal activity* (2nd ed.). New York, NY: Springer.
- Boucsein, W., Fowles, D. C., Grimnes, S., Ben-Shakhar, G., Roth, W. T., Dawson, M. E., & Filion, D. L. (2012). Publication recommendations for electrodermal measurements. *Psychophysiology*, 49, 1017–1034. doi:10.1111/j.1469-8986.2012.01384.x
- Bradley, M. M., Miccoli, L., Escrig, M. A., & Lang, P. J. (2008). The pupil as a measure of emotional arousal and autonomic activation. *Psychophysiology*, 45, 602–607. doi:10.1111/j.1469-8986.2008.00654.x
- Brainard, D. H. (1997). The psychophysics toolbox. *Spatial Vision*, 10, 433–436. doi:10.1163/156856897X00357
- Cacioppo, J., & Tassinary, L. G. (1990). Inferring psychological significance from physiological signals. *American Psychologist*, 45, 16–28. doi:10.1037/0003-066X.45.1.16
- Czaja, S. J., & Sharit, J. (1993). Stress reactions to computer-interactive tasks as a function of task structure and individual differences. *International Journal of Human-Computer Interaction*, 5, 1–22. doi:10.1080/10447319309526053
- Dawson, M. E., Schell, A. M., & Filion, D. L. (2000). The electrodermal system. In J. T. Cacioppo, L. G. Tassinary, & G. G. Berntson (Eds.), *Handbook of psychophysiology* (2nd ed., pp. 200–223). Cambridge, UK: Cambridge University Press.
- Dennerlein, J., Becker, T., Johnson, P., Reynolds, C., & Picard, R. (2003). Frustrating computer users increases exposure to physical factors. *Proceedings of the International Ergonomics Association*, 24–29.
- Di Stasi, L., Catena, A., Cañas, J., Macknik, S. L., & Martinez-Conde, S. (2013). Saccadic velocity as an arousal index in naturalistic tasks. *Neuroscience and Biobehavioral Reviews*, 37, 968–975. doi:10.1016/j.neubiorev.2013.03.011
- Ellis, C. J. (1981). The pupillary light reflex in normal subjects. *British Journal of Ophthalmology*, 65, 754–759. doi:10.1136/bjo.65.11.754
- Fawcett, T. (2006). An introduction to ROC analysis. *Pattern Recognition Letters*, 27, 861–874. doi:10.1016/j.patrec.2005.10.010
- Fujigaki, Y., & Mori, Kazuko (1997). Longitudinal study of work stress among information system professionals. *International Journal of Human-Computer Interaction*, 9, 369–381. doi:10.1207/s15327590ijhc0904_3
- Gitelman, D. R. (2002). ILAB: A program for postexperimental eye movement analysis. *Behavior Research Methods, Instruments, & Computers*, 34, 605–612. doi:10.3758/BF03195488
- Goldwater, B.C. (1972). Psychological significance of pupillary movements. *Psychological Bulletin*, 77, 340–355. doi:10.1037/h0032456
- Granholm, E., & Steinhauer, S. R. (2004). Pupillometric measures of cognitive and emotional processes. *International Journal of Psychophysiology*, 52, 1–6. doi:10.1016/j.ijpsycho.2003.12.001
- Granholm, E., & Verney, S. P. (2004). Pupillary responses and attentional allocation problems on the backward masking task in schizophrenia. *International Journal of Psychophysiology*, 52, 37–51. doi:10.1016/j.ijpsycho.2003.12.004
- Hamid, N. A., Nawi, N. M., & Ghazali, R. (2011). The effect of adaptive gain and adaptive momentum in improving training time of gradient descent

- back propagation algorithm on classification problems. *International Journal on Advanced Science, Engineering and Information Technology*, 1, 178–184.
- Holmqvist, K., Nyström, M., Andersson, R., Dewhurst, R., Jarodzka, H., & van de Weijer, J. (2010). *Eye tracking: A comprehensive guide to methods and measures*. New York, NY: Oxford University Press.
- ISO 26022, 2010. Road vehicles—Ergonomic aspects of transport information and control systems - Simulated lane change test to assess in-vehicle secondary task demand. ISO/TC 22/SC 13.
- Jainta, S., & Baccino, T. (2010). Analyzing the pupil response due to increased cognitive demand: An independent component analysis study. *International Journal of Psychophysiology*, 77, 1–7. doi:10.1016/j.ijpsycho.2010.03.008
- Janisse, M. P. (1977) *Pupillometry: The psychology of the pupillary response*. Washington DC: Hemisphere.
- Kleiner, M., Brainard, D. H., & Pelli, D. G. (2007). *What's new in Psychtoolbox-3?* Perception 36 ECPV Abstract Supplement.
- Klingner, J. (2010). Fixation-aligned pupillary response averaging. In *Proceedings of the 2010 Symposium on Eye-Tracking Research & Applications* (pp. 275–282). New York, NY: ACM Press.
- Klingner, J., Kumar, R., & Hanrahan, P. (2008). Measuring the task-evoked pupillary response with a remote eye tracker. In *Proceedings of the 2008 Symposium on Eye-Tracking Research & Applications*, pp. 69–72. New York, NY: ACM Press.
- Kuchinke, L., Vo, M. L. H., Hofmann, M., & Jacobs, A. M. (2007). Pupillary responses during lexical decisions vary with word frequency but not emotional valence. *International Journal of Psychophysiology*, 65, 132–140.
- Kuhlmann, J., & Böttcher, M. (1999). *Pupillography: Principles, methods and applications*. München, Germany: W. Zuckschwerdt Verlag.
- Lanting, P., Bos, J. E., Aartsen, J., Schuman, L., Reichert-Thoen, J., & Heimans, J. J. (1990). Assessment of pupillary light reflex latency and darkness adapted pupil size in control subjects and in diabetic patients with and without cardiovascular autonomic neuropathy. *Journal of Neurology, Neurosurgery, and Psychiatry*, 53, 912–914. doi:10.1136/jnnp.53.10.912
- Lew, R., Dyre, B. P., Werner, S., Wotring, B., & Tran, T. (2008). Exploring the potential of Short-Time Fourier Transforms for analyzing skin conductance and pupillometry in real-time applications. In *Proceedings of the Human Factors and Ergonomics Society 52nd Annual Meeting* (pp. 1536–1540). Santa Monica, CA: Human Factors and Ergonomics Society.
- Loewenfeld, I., & Lowenstein, O. (1993). *The pupil: Anatomy, physiology, and clinical applications* (Vol. I). Ames: Iowa State University.
- Lüdtke, H., Wilhelm, B., Adler, M., Schaeffel, F., & Wilhelm, H. (1998). Mathematical procedures in data recording and processing of pupillary fatigue waves. *Vision Research*, 38, 2889–2896.
- Mallat, S. G. (1989). A theory for multiresolution signal decomposition: The wavelet representation. *IEEE Transactions on Pattern Analysis and Machine Intelligence*, 11, 674–693.
- Mauss, I. B., & Robinson, M. D. (2009). Measures of emotion: A review. *Cognition and Emotion*, 23, 209–237. doi:10.1080/02699930802204677
- Marshall, S. P. (2000). Method and apparatus for eye tracking and monitoring pupil dilation to evaluate cognitive activity. US Patent No. 6,090,051.
- Marshall, S. P. (2002). The Index of Cognitive Activity: Measuring cognitive workload. *Proceedings of the 7th Conference on Human Factors and Power Plants*, 7.5–7.9.
- Minin, L., Benedetto, S., Pedrotti, M., Re, A., & Montanari, R. (2011). Measuring the effects of visual demand on lateral deviation: A comparison among driver's performance indicators. *Applied Ergonomics*, 43, 486–492.
- Minu, K. K., Lineesh, M. C., & Jessy John, C. (2010). Wavelet neural networks for nonlinear time series analysis. *Applied Mathematical Sciences*, 4, 2485–2495.
- Mitsopoulos-Rubens, E., Trotter, M. J., & Lenné, M. G. (2011). Effects on driving performance of interacting with an in-vehicle music player: A comparison of three interface layout concepts for information presentation. *Applied Ergonomics*, 42, 583–591.
- More, J. J. (1978). The Levenberg-Marquardt algorithm: Implementation and theory. *Numerical Analysis*, 630, 105–116.
- Nakayama, M. (2006). Influence of blink on pupillary indices. *Biomedical Circuits and Systems Conference*, 2006, 29–32. IEEE Conference Publications.
- Nakayama, M., & Shimizu, Y. (2002). An estimation model of pupil size for 'Blink artifact' and its applications. In M. Verleysen, M. (Ed.), *10th European Symposium on Artificial Neural Networks* (pp. 251–256). Bruges, Belgium: D-side publications.
- Nakayama, M., & Shimizu, Y. (2004). Frequency analysis of task evoked pupillary responses and eye-movement. In A. T. Duchowsky & R. Vertegaal (Eds.), *Eye-Tracking Research & Applications Symposium 2004* (pp. 71–76). New York, NY: ACM Press.
- Nakayama, M., Yamamoto, K., & Kobayashi, F. (2012). Estimation of sleepiness using pupillary response and its frequency components. *International Journal of Bioinformatics Research and Applications*, 8, 342–365.
- Nhan, B. R., & Chau, T. (2010). Classifying affective states using thermal infrared imaging of the human face. *IEEE Transactions on Biomedical Engineering*, 57, 979–987. doi:10.1109/TBME.2009.2035926
- Palinko O., & Kun, A. L. (2011). Exploring the influence of light and cognitive load on pupil diameter in driving simulator studies. In *Proceedings of the Sixth International Driving Symposium on Human Factors in Driver Assessment, Training and Vehicle Design* (pp. 329–336). Iowa City: Public Policy Center, University of Iowa.
- Palinko O., & Kun, A. L. (2012). Exploring the effects of visual cognitive load and illumination on pupil diameter in driving simulators. In *Proceedings of the 2012 Symposium on Eye-Tracking Research & Applications* (pp. 413–416). New York, NY: ACM Press.
- Palinko, O., Kun, A. L., Shyrov, A., & Heeman, P. (2010). Estimating cognitive load using remote eye tracking in a driving simulator. In *Proceedings of the 2010 Symposium on Eye-Tracking Research & Applications* (pp. 141–144). New York, NY: ACM Press.
- Partala, T., & Surakka, V. (2003). Pupil size variation as an indicator of affective processing. *International Journal of Human-Computer Studies*, 59, 185–198.
- Pedrotti, M., Lei, S., Dzaack, J., & Rötting, M. (2011). A data-driven algorithm for offline pupil signal preprocessing and eyeblink detection in low-speed eye-tracking protocols. *Behavior Research Methods*, 43, 372–383.
- Pelli, D. G. (1997). The VideoToolbox software for visual psychophysics: Transforming numbers into movies. *Spatial Vision*, 10, 437–442.
- Pinzon-Morales, R. D., & Hirata, Y. (2012). Customization of wavelet function for pupil fluctuation analysis to evaluate levels of sleepiness. In *Proceedings of the 11th International Conference on Telecommunications and Informatics, Proceedings of the 11th International Conference on Signal Processing* (pp. 115–120). Stevens Point, WI: World Scientific and Engineering Academy and Society.
- Ren, P., Barreto, A., Gao, Y., & Adjouadi, M. (2013). Affective assessment by digital processing of the pupil diameter. *IEEE Transactions on Affective Computing*, 4, 2–14.
- Sato, K., Kang, W.H., Saga, K., & Sato, K. T. (1989). Biology of sweat glands and their disorders. I. Normal sweat gland function. *Journal of the American Academy of Dermatology*, 20, 537–563.
- Sauter, S. L. (1991). Job stress and human-computer interaction. *International Journal of Human-Computer Interaction*, 4(3), 3–4.
- Schweitzer, M. B., & Paulhan, I. (1990). *Manuel pour l'inventaire d'anxiété Trait-État* (Forme Y). Laboratoire de Psychologie de la Santé, Université de Bordeaux II. Bordeaux, France.
- Shastri, D., Merla, A., Tsiamyrtzis, P., & Pavlidis, I. (2009). Imaging facial signs of neurophysiological responses. *IEEE Transactions on Biomedical Engineering*, 56, 477–484.
- Shi, B., Moloney, K. P., Pan, Y., Leonard, V. K., Vidakovic, B., Jacko, J. A., & Sainfort, F. (2012). Wavelet classification of high frequency pupillary responses. *Journal of Statistical Computation and Simulation*, 76, 431–446.
- Spielberger, C. D., Gorsuch, R. L., Lushene, R., Vagg, P. R., & Jacobs, G. A. (1983). *Manual for the State-Trait Anxiety Inventory*. Palo Alto, CA: Consulting Psychologists Press.
- Tournois, J., Mesnil, F., & Kop, J. L. (2000). Autotracherie et hétérotracherie: Un instrument de mesure de la désirabilité sociale. [Self-deception and other-deception: A social desirability measuring tool]. *Revue Européenne de Psychologie Appliquée / European Review of Applied Psychology*, 50, 219–232.
- Van den Broek, E. L., Janssen, J. H., & Westerink, J. H. D. M. (2009). Guidelines for Affective Signal Processing (ASP): From lab to life.

- In *Proceedings of the IEEE 3rd international conference on affective computing and intelligent interaction (ACII)*, Vol. 1, pp. 704–709. Amsterdam, the Netherlands: IEEE Press.
- Verney, S. P., Granholm, E., & Marshall, S. P. (2004). Pupillary responses on the visual backward masking task reflect general cognitive ability. *International Journal of Psychophysiology*, 52, 23–36.
- Vo, M. L. H., Jacobs, A. M., Kuchinke, L., Hofmann, M., Conrad, M., Schacht, A., & Hutzler, F. (2008). The coupling of emotion and cognition in the eye: Introducing the pupil old/new effect. *Psychophysiology*, 45, 130–140.
- Watson, A. B., & Yellot, J. I. (2012). A unified formula for light-adapted pupil size. *Journal of Vision*, 12(10), 1–16.
- Widrow, B., Gupta, N. K., & Maitra, S. (1973). Punish/reward: learning with a critic in adaptive threshold systems. *IEEE Transactions on Systems, Man and Cybernetics*, SMC-3, 455–465.
- Wyatt, H. J. (2010). The human pupil and the use of video-based eyetrackers. *Vision Research*, 50, 1982–1988.
- Zhai, J., & Barreto, A. (2006). Stress detection in computer users based on digital signal processing of noninvasive physiological variables. *Engineering in Medicine and Biology Society, 2006. EMBS'06. 28th Annual International Conference of the IEEE*, 1355–1358.

ABOUT THE AUTHORS

Marco Pedrotti received his Ph.D. in Applied Psychology and Ergonomics from the Università di Torino in 2011. He is currently a post-doc researcher at the LUTIN lab (<http://www.lutin-userlab.fr>) for Université Pierre et Marie Curie, Paris. His research focuses on unobtrusive sensing of emotions and operator's state.

Mohammad Ali Mirzaei is a Ph.D. Student in Arts et Métiers ParisTech, France. He received his MS in micro-electronics engineering (signal processing and SoC systems) in Imperial College, London. His research focuses on signal/image processing and real-time systems.

Adrien Tedesco is a Ph.D. Student in the Laboratoire d'étude des mécanismes cognitifs at Université Lyon 2. He works as research engineer for Scientific Brain Training (Villeurbanne, France) and coordinator of the MASSAI project (www.projet-massai.com). His research investigates measures and effects of anxiety on cognitive performance.

Jean-Rémy Chardonnet received his Ph.D. degree in robotics from the Université de Montpellier II, France, in 2009. He was then with INRIA Grenoble, France. He is currently Assistant Professor at Arts et Métiers ParisTech and CNRS Le2i Institut Image, Chalon-sur-Saône, France. His research interests include virtual reality and multimodal interaction.

Frédéric Mérienne is full professor at Arts et Métiers ParisTech and head of the research team in Virtual Immersion of the Le2i laboratory (Burgundy University, Arts et Métiers ParisTech, CNRS). His research topics concern multisensory immersive techniques for interacting with a digital mock-up.

Simone Benedetto received his Ph.D. in Applied Psychology and Ergonomics from the Università di Torino in 2011. He was then with IFSTTAR, France. He is currently a post-doc researcher at the LUTIN lab (<http://www.lutin-userlab.fr>) for Université Paris 8. His research is focused on cognitive ergonomics.

Thierry Baccino is full professor of Cognitive Psychology at Université Paris 8 and scientific director of the LUTIN lab (<http://www.lutin-userlab.fr>). His research aims at interpreting and modeling visual search in real-life contexts such as reading, information retrieval, and image viewing.